Polymer Composites

WILEY | spe INSPIRING PLASTICS PROFESSIONALS

RESEARCH ARTICLE OPEN ACCESS

Linking Process-Induced Degradation to Mechanical Property Deterioration in Flax Fiber–Reinforced Bio-Polymer Matrix Composites

Dimitrios Apostolidis | Prajwal Jayaraman | Clemens A. Dransfeld | Baris Kumru | Niklas Lorenz

Aerospace Structures & Materials Department, Faculty of Aerospace Engineering, Delft University of Technology, Delft, HS, the Netherlands

Correspondence: Niklas Lorenz (n.lorenz@tudelft.nl)

Received: 21 September 2025 | **Revised:** 9 November 2025 | **Accepted:** 29 November 2025

Keywords: biobased composites | chemical degradation | composite manufacturing | flax fibers | mechanical properties | PA11 | thermal degradation

ABSTRACT

The drawback of biobased polymer matrix composites (PMCs) is their limited temperature stability, resulting from degradation, which restricts their processability in established composite manufacturing processes requiring elevated temperatures. These key issues not only affect the mechanical properties but ultimately limit the utilization of flax fibers as fiber reinforcement in PMCs. In this study, kinetic models for the thermal degradation of flax fibers and PA11 are derived and combined with a model for thermo-chemical fiber degradation. Selective degradation of the fibers and mechanical testing establishes a link between degradation and the accompanying deterioration of the mechanical performance. The deterioration of flax fiber mechanical properties under concurrent thermal and thermo-chemical degradation is primarily governed by the thermos-chemical contribution (chain scission) up to 3% thermal degradation, beyond which the influence of thermal degradation becomes evident. Even 1% thermal degradation of flax fibers results in a pronounced reduction in their mechanical performance. In contrast, equal degradation values enhance the PMCs' strength, which may be attributed to improved fiber-matrix interactions. Compiling results into processing maps establishes a framework for designing tailored processing of temperature-sensitive materials, offering transfer opportunities to individual processing conditions and heat treatments, enabling broader research on bio-based PMCs.

1 | Introduction

Bio-based polymers with natural fibers are promising candidates for transforming petrol-based polymer matrix composites (PMCs) for engineering applications into more sustainable alternatives. Replacing petroleum with biobased feedstocks for polymer synthesis directly contributes to today's green chemistry of renewable platform chemicals, becoming increasingly critical for both ecological and economic concerns [1]. Additionally, natural fibers have the potential to replace glass as a reinforcement in PMCs, thereby offering a more sustainable alternative [2, 3]. In this light, cellulosic fibers are of great importance due to their characteristics, including low cost and low density, non-toxicity, acoustic insulation, and the ability to enhance the strength and stiffness of polymeric matrices [2–5]. Particularly, flax fibers excel due to their superior mechanical characteristics, which are attributed to their high concentration of cellulose (60 wt% – 70 wt%), crystallinity (50%–90%), and small microfibrillar angles (< 10°) [5].

One key challenge for the application of natural fibers in thermoplastic PMCs is minimizing the thermal degradation of the hemicellulose and cellulose materials that may occur during the hot processing of the composite [6–8]. Specifically, temperature and dwelling times during manufacturing represent critical parameters that govern the thermal degradation behavior of both fiber and polymer matrix constituents. On the one hand, the imposed temperature during the consolidation step must exceed

Highlights

- Model-free kinetics accurately model the degradation of flax fiber and PA11.
- Thermal degradation is linked with the mechanical performance of flax fibers and their composites.
- Thermal degradations up to 1% yield improved composite strength.
- TTT diagrams can be utilized as a framework to outline distinct processing regimes.

the polymer matrix melting temperature to ensure a low melt viscosity, thereby promoting adequate penetration and impregnation of the fibrous reinforcement. On the other hand, the integral processing temperature should be minimized, and the residual time should be as short as possible to mitigate undesired thermal and thermo-chemical degradation, which can lead to a loss of mechanical performance. This results in a constrained processing window, where optimization is essential to achieve adequate fiber-matrix consolidation without compromising the structural integrity and mechanical performance of the resulting PMC.

Since bio-based fibers [9–14] suffer from this thermal stability issue compared with synthetic fibers, the effect has increasingly been focused on in the literature. Various studies indicate that thermal degradation is predominantly determined by fiber properties such as chemical composition, moisture content, density, and crystallinity [15–18]. Degradation of natural fibers is considered a three stage process consisting of initial weight loss by dying and removal of water up to 150°C (i), devolatilization of the major component of the fiber, like hemicellulose, cellulose, and lignin in temperature range of 200°C–435°C (ii) and finally the formation of char by decomposition of lignin contents at temperatures above 440°C (iii) [19]. Step (ii) is accompanied by deterioration of the mechanical properties [4, 20, 21]. For flax fibers, even at lower temperatures (below 300°C), the presence of water can accelerate degradation, and degradation can be autocatalyzed by CO_2 and carboxylic acids [14]. Furthermore, the formation of free radicals has already been observed at temperatures between 100°C and 160°C, which yields the formation of hydroperoxide groups and therefore contributes to the depolymerization of cellulose through bond scission [14]. Even the drying process can cause irreversible changes in the fiber structure, making the fibers more brittle [21].

Thus, the degradation of the fiber constituents constrains the processing window of PMCs, and the thermal degradation of flax fibers after submitting to isothermal dwellings ranging from 170°C to 250°C has been studied in [9, 10, 14, 22–25]. Temperatures below 170°C have only a slight effect on the mechanical properties (tenacity) of the fiber and the degree of polymerization [10]. Additionally, isothermal dwellings above 180°C for one hour are accompanied by a significant deterioration in fiber tensile strength [22, 25] and an increase in failure strain [22]. After exposing elementary flax fibers to isothermal dwellings at 190°C, 210°C, and 250°C for 8 min, the modulus and strength of elemental flax fibers start to decrease above 190°C, gradually [24]. Besides that, the tenacity of flax fibers has been shown to decrease linearly with the degree of polymerization [10, 26]. Furthermore, Fourier transform infrared spectrometry reveals that the band in the 1750–1700 cm^{-1} region changes, indicating that the hemicelluloses in the fibers have degraded during isothermal dwellings at 200°C [23]. Conversely, an increased strength of the fibers at temperatures of 180°C was observed and attributed to the crosslinking of the cellulose. However, a rapid decrease in strength was observed after submitting the fibers to 5 min isothermal dwellings at 220°C, which the authors claim is the maximum processing temperature [9]. It is noteworthy that in the majority of studies, the effect of a specific temperature history (i.e., time–temperature pairs) on the resulting fiber properties is typically characterized, rather than the apparent thermal or thermo-chemical material degradation.

The mechanisms of thermal degradation in polymeric fibers and polymers are inherently complex [27]. Molecular scission of the polymer chain degrades the material and alters the molecular weight distribution [27, 28]. Volatile products from hemicellulose, cellulose, and lignin degradation may escape from the polymer, resulting in a reduction in mass. The thermal degradation of vegetal fibers undergoes a heterogeneous and complex process transitioning from diffusion to random nucleation mechanisms at higher conversion rates [2, 18]. Thermogravimetric analysis provides a pathway for analyzing the macroscopic kinetics of these thermally induced degradation processes. Applying isoconversional methods represents a well-established approach to describing thermally activated processes such as chemical reactions [28, 29] and enables the precise description of the thermal degradation of various polymeric materials [14, 27, 30, 31] and composites [32, 33]. Indeed, these methods do not allow the isolation of elementary reactions but provide an average measure of the conversion rate, involving several superimposed activation energies [34], allowing the precise prediction of the thermal degradation process based on the mass loss [27]. For bio-based fibers, modeling the global reactions involves typical activation energies of hemicellulose (105–111 kJ mol^{-1}), cellulose (195–213 kJ mol^{-1}), and lignin (35–65 kJ mol^{-1}) [30]. For flax fibers with different retting degrees, activation energies ranging from 75.7 to 202 kJ mol^{-1} are reported [14, 25]. The degradation behavior of bio-based polyamide 11 (PA11) was investigated in [31], revealing a two-step degradation process with activation energies of 92 kJ mol^{-1} and 272 kJ mol^{-1}, respectively. Notably, there was no noticeable mass loss at temperatures below 325°C. Therefore, isoconversional methods are convincing because they describe degradation kinetics without knowing the exact mechanisms, yet still provide meaningful mechanistic insights and kinetic predictions. They thus offer a way to describe the distinct degradation state resulting from arbitrary dwelling times and temperatures.

In addition to evaluating the fiber and matrix components individually, PMCs reinforced with continuous bio-based fibers have been studied for their thermal degradation behavior with a focus on identifying specific processing windows that minimize this degradation [6, 21, 24, 35–37]. In general, thermoset materials are considered beneficial for circumventing degradation during high-temperature processing [3], given that the curing temperatures are significantly lower than the melt processing temperatures of thermoplastic matrix

materials [38]. Therefore, the low thermal stability of bio-based fibers represents a significant limitation for the composite manufacturing process [21, 39]. Due to its relatively low melting temperature and the balance of cost and performance, polypropylene (PP) is a favorable choice for PP/flax composites with continuous fiber reinforcements [35]. The selected temperature and dwelling time have a significant influence on the mechanical performance and aesthetics of Flax/PP composites [35, 36], with prolonged exposures above 175°C already significantly deteriorating the tensile properties [35]. Compared with PP, the higher viscosities and melting points of PA6 and PA11 make it more challenging to establish an appropriate processing window when manufacturing PMC with flax reinforcement. By investigating the influence of processing temperature and time on the tensile and flexural behavior of flax/PA6 composites, the authors conclude that significant deterioration of mechanical performance (up to a 64% loss in tensile strength) occurs as consolidation temperatures are increased to 250°C for 5 min [21]. Flax/PA11 bio-composites with high mechanical performance are manufactured in [24]. The processing window is defined based on studies of the thermal degradation (distinct time–temperature profiles) of elementary flax fibers, which highlight significant deterioration of mechanical performance when processing temperatures are above 210°C. Additionally, the authors demonstrate that using the rule of mixtures, combined with the strength of elementary fibers, enables the precise prediction of laminate properties. The effect of the molding temperature and time on the mechanical properties of flax/PLA bio-composites during consolidation in compression molding is considered in [37]. As the molding temperature and time increase, the mechanical properties, especially the strength of the composite, decrease by up to 35%.

Optimized process boundaries for flax/PLA bio-composites are derived in [6]. The authors employ a multi-physical modeling approach that includes heating, yarn impregnation, and degradation (thermal and chain scission) to identify a distinct processing window for the isothermal processing of flax/PLA bio-composites. In the case studied, thermos-chemical degradation by chain scission of the fiber and matrix sets the upper limit, while the time required for the melt to penetrate the yarn defines the lower limit for the allowable residual time during hot pressing. Sticking to favorable processing conditions enables the manufacture of laminates with elevated tensile strength. Additionally, a relationship between the degree of polymerization (derived from the thermal history of the materials during processing) and mechanical properties is established and applied to calculate the tensile strength of a flax/PLA bio-composite [40]. However, thermal material degradation (indicated by a mass loss) is not considered the main concern for the production process.

While practitioners working with bio-composites are undoubtedly aware of the degradation issue, there have been only a few attempts to quantitatively map thermal process boundaries for film impregnation of bio-composites, for example, by means of Time–temperature-transformation (TTT) diagrams, considering both thermal degradation and thermo-chemical degradation (chain scission) of flax fibers. A precise understanding of the degradation processes is crucial for selecting feasible processing windows and recycling routes. Indeed, existing models for the thermal degradation process of flax fibers [6, 14, 41], which assume constant activation energies and pre-exponential factors, allow the prediction of temperature and time couples for specific isoconversional values; however, they have been applied to strictly isothermal temperature profiles, which rarely exist in reality.

The aim is to develop processing maps that support users in tailoring processing windows to categorically avoid deterioration in mechanical performance during the processing of PMCs. Therefore, we first model both thermal and thermo-chemical degradation, also for an arbitrary temperature profile. These models are used to selectively degrade flax fibers and flax-PMCs manufactured in the film impregnation process. Subsequent mechanical testing of selectively degraded specimens reveals a correlation between thermal and thermo-chemical degradation and their effect on mechanical performance. Finally, we compile the data into processing maps that indicate a suitable processing window for the manufacture of flax-PMC, accounting for tolerable deterioration in mechanical properties.

2 | Experimental

2.1 | Materials

Rilsan Polyamide 11 (PA11) granulate, obtained from castor oil, was provided by Arkema S.A., France. Its outstanding chemical and thermal resistance has led to its widespread use in high-performance components, particularly within aerospace applications, making it a promising green alternative to conventional synthetic polymers. Continuous non-crimp unidirectional rolls and flax fabric AmpliTex 5025 with a grammage of 280 g/m^2 were purchased from Bcomp Ltd., Switzerland, and used as received. The external mold release agent Marbocote 227, from Marbocote Ltd., UK, the sealant type Cytec LTS90B, UK, and Wrightlon 8400 nylon film from Airtech, Luxembourg, were used for the composite manufacturing process.

2.2 | Modeling Approach

Thermogravimetric analysis (TGA) was performed using a TGA 4000 from PerkinElmer Inc., USA. All measurements were performed at an air flow rate of 20 mL/min. Samples with mass varying from 15 to 25 mg were degraded in a range from 25°C to 900°C with heating rates of 5,10,15, 25 and 50 K/min. As is also standard practice in processing, flax fibers and PA11 are pre-dried at 100°C for 1 h to minimize weight loss, which occurs due to the release of moisture and low-molecular-weight compounds, such as extractives. Additionally, previous drying of the fibers may increase the apparent thermal stability of the vegetal fibers [2]. Besides that, cryo-milled fiber-polymer mixtures with a fiber weight content of 50 wt. % are submitted to heating ramps of 15 K/min to validate the applicability of the rule of mixtures.

Model-free kinetics based on TGA represent an established approach to modeling the degradation of fiber [2, 14, 42], polymer matrix [27, 32] and PMCs [4, 43]. The degradation of fiber and

polymer matrix material exhibits complex degradation kinetics. TGA registers the mass change of the sample with time or temperature at the specified gas environment (in our case, air) and heating rate. The actual weight $m(t)$ is then converted into conversion $\alpha(t)$:

$$\alpha(t) = \frac{m_0 - m(t)}{m_\infty - m_0}, \tag{1}$$

while m_0 and m_∞ represent the initial and final mass of the sample. By introducing a generalized kinetic equation Equation (1), the degradation rate $\frac{d\alpha}{dt}$ is described by a temperature-dependent rate constant $k(T)$ and a mass-dependent reaction model $f(\alpha)$ [27]:

$$\frac{d\alpha}{dt} = k(T)f(\alpha). \tag{2}$$

While assuming that $k(T)$ follows Arrhenius law and applying a constant heating rate β, the degradation rate $\frac{d\alpha}{dt}$ can be numerically calculated from the temperature and conversion data according to:

$$\beta\frac{d\alpha}{dT} = \exp\left(\frac{-E}{RT}\right)f(\alpha), \tag{3}$$

where $\beta = \frac{dT}{dt}$, represents the heating rate, E the apparent activation energy of the degradation process, and R the universal gas constant. The mathematical manipulations of Equation (3) enables the determination of kinetic triples (E, A and $f(\alpha)$) utilizing the degradation data obtained from the TGA measurements at multiple heating rates.

Various analytical and computational methods have been developed to approximate data derived from dynamic TGA measurements into an appropriate mathematical expression. Isoconversional methods provide meaningful insights into mechanistic analysis, detecting governing degradation mechanisms [44, 45]. The isoconversional principle states that the degradation rate $\frac{d\alpha}{dt}$ at a certain isoconversional value is solely a function of temperature [28, 46]:

$$\left[\frac{\partial \ln\left(\frac{d\alpha}{dt}\right)}{\partial T^{-1}}\right]_\alpha = -\frac{E_\alpha}{R}, \tag{4}$$

whereas E_α is the apparent activation energy for a conversion α, and R is the universal gas constant. Based on Equation (5) a model-free value of the apparent activation energy can be estimated for each α value. The applied isoconversional methods can be grouped into integral (Kissinger [47], Ozawa-Flyn-Wall [48, 49] and Vyazovkin [50]) and differential methods, such as Friedman [32]. Within the present work, we utilize Friedman's method [32]:

$$\ln\left(\frac{d\alpha}{dt}\right)_{\alpha,i} = ln\left[A_\alpha f(\alpha)\right] - \frac{E_\alpha}{RT_{\alpha,i}}. \tag{5}$$

Applying this method requires knowledge of the degradation rate $\left(\frac{d\alpha}{dt}\right)_{\alpha,i}$ and the corresponding temperature $T_{\alpha,i}$ for a specific extent of conversion α across i temperature programs utilized [44]. Within the present work, E_α is calculated for α ranging from 0.001–0.100 within steps of 0.001 yielding $N = 100$ discrete steps. The threshold of 0.1 forms the ultimate upper boundary for the fiber degradation during the processing of bio-based PMC in compression molding [6], which is accompanied by ~10% degradation of the composite's tensile strength.

The five temperature programs include heating with constant heating rates β_i of 5, 10, 5, 20, 50 K/min, which represent temperatures apparently occurring during film impregnation of PMCs. For each β_i, the $\left(\frac{d\alpha}{dt}\right)_{\alpha,i}$ and $T_{\alpha,i}$ values are determined. As the term $ln\left[A_\alpha f(\alpha)\right]$ remains constant for a particular value of α, the left-hand side of Equation (5) depends linearly on the reciprocal temperature. Taking advantage of this linear correlation, the effective E_α can be calculated from the slope while $A_\alpha f(\alpha)$ represents the y-intercept, respectively. By applying Friedman's differential method, we obtain the activation energy and kinetic parameters conversion for N discrete points within the selected α range.

To solve this problem for an arbitrary temperature program $T(t)$, we apply the approach suggested *by Farjas and Roura* [51] and discretize the dependence of temperature on time into constant time intervals, Δt, so that $t_k = k\,\Delta t$ where k is a natural number and $T_k = T(t_k)$. The method is derived directly from Equation (2) by replacing the differentials by increments yielding:

$$\alpha_{k+1} = \alpha_k + A_{\alpha,k} f(\alpha_k) \exp\left(\frac{-E_{\alpha,k}}{RT_k}\right)\Delta t. \tag{6}$$

Interpolation of distinct pairs of activation energy and preexponential factors with defined Δt of 0.1 s. $E_{\alpha,k}$ and $A_{\alpha,k} f(\alpha_k)$ in Equation (6) are interpolated from discrete sets of $E_{\alpha,j}$ and $A_{\alpha,j} f(\alpha_j)$ [52] with j rangig from 1 to N+1 and covering an α range of 0.0–0.10. Following the methodology outlined, this manuscript determines kinetic evolutions through direct time integration of the transformation rate. This approach has been employed to predict the kinetics of decomposition under isothermal and dynamic conditions.

The fiber materials were selectively degraded by submitting to elevated temperature dwellings in a convection oven (Vötsch VTL Vötsch GmbH, Germany). After preheating the oven for 1 h, the fibers, specifically PMC, are subjected to the time–temperature histories provided in Table 1. An analytical consideration of 1-D heat conduction in the radial and laminated thickness directions of fibers indicated a negligible effect of in-thickness temperature gradients and close-to-instantaneous heating (cf. section 1 in SI, Figure S1). Still, for the PMC laminates, we increase the dwelling times by 200 s to account for the delayed heating of the thicker cross-section (Figure S2). Due to the projected low processing temperatures and short residual times, degradation of the PA11 matrix material may be considered negligible, as no significant impact of the thermal history on mechanical performance was observed during the initial mechanical recycling and remolding at temperatures of up to 235°C [53]. Still, the thermal degradation of neat PA 11 and PMC is also investigated to confirm that assumption and explore the effect of interactions within the mixture.

In addition to thermal degradation, cellulose chains undergo chain scission (thermo-chemical degradation) at elevated temperatures, similar to that of polymeric matrix materials. While

TABLE 1 | Imposed time–temperature profiles for selective thermal degradation α of fiber bundles and FRP laminates and corresponding thermal and thermo-chemical degradation.

α	κ	Temperature [°C]	Time [min]
0.01	0.49	205	19.5
0.02	0.57	218	19.2
0.03	0.72	240	22.5
0.05	0.77	245	25.4
0.06	0.79	250	25.7
0.07	0.80	255	24.1

the overall weight remains constant, the average molecular weight of the polymer decreases. For jute and flax fibers, a thermo-chemical degradation process parameter $\kappa(t)$ has been introduced to identify the extent of chain scission during the processing [10]:

$$\kappa(t) = \frac{DP_0 - DP(t)}{DP_0 - 1}, \tag{7}$$

while DP represents the degree of polymerization, describing the number-averaged molar mass divided by the molar mass of a monomer unit during the isothermal dwellings and DP_0 the dimensionless initial degree of polymerization is set to 1505 for flax fibers [6, 10]. It should be emphasized that a single distinct degree of polymerization is atypical for natural fibers, which generally exhibit a broader property distribution and may therefore differ from the flax fibers investigated in this study. To quantify the chain scission effect, the chemical rate equation can be expressed in terms of N, the total number of bonds between the monomer units [26]:

$$N = 1 - \frac{1}{DP}. \tag{8}$$

Assuming the random scission of bonds in a linear chain polymer follows a first-order kinetics rate law, Equation (8) can be written as [26]:

$$\frac{dN}{dt} = K \times N, \tag{9}$$

with K representing the rate constant. Utilizing the approach suggested in [6] with a temperature-dependent rate constant exhibiting Arrhenius-like behavior, the scission rate $\frac{dN}{dt}$ can be dismantled by the following differential equation:

$$\frac{dN}{dt} = A \exp\left(-\frac{E_a}{RT(t)}\right) \times N, \tag{10}$$

with $E_a = 50.5$ KJ/mol and $A = -0.178\,\mathrm{s}^{-1}$ being constant [6]. By applying Euler integration, similar to Equation (6), the total number of bonds N, excluding any crystallinity effect and non-covalent interactions, may be calculated for an arbitrary temperature profile T_k:

$$N_{k+1} = N_k + A \exp\left(-\frac{E_a}{RT_k}\right) \Delta t. \tag{11}$$

Considering Equation (8) with $N_0 = 1 - \frac{1}{DP_0}$ and $N_k = 1 - \frac{1}{(1-\kappa_k)\cdot DP_0}$, the degradation cause by chain scission κ_k is calculated at each step k utilizing Equation (12).

$$\kappa_k = 1 - \frac{1}{(1 - N_k)\cdot DP_0}. \tag{12}$$

In conclusion, by applying Equation (6) with parameters obtained from TGA experiments, Equation (11), and Equation (12) in combination with literature values [6], the thermal degradation a and thermo-chemical degradation κ can be determined for arbitrary temperature profiles.

2.3 | Mechanical Testing of Flax Fiber Bundles

For the fiber bundle testing, single fiber bundles ($d = 0.1$–0.46 mm) were mounted on paper tabs using adhesive, with a gauge length of 80 mm (Figure S6) according to ASTM C1557 standard [54]. Only individual fibers were selected and confirmed under a microscope. Individual fiber diameters were measured via optical microscopy (VR 5000 digital microscope from Keyence Corp., Japan, with a 100 × magnification) before testing, and the average of three diameters was used to calculate the cross-sectional area for stress calculations, thereby avoiding distortions from extreme values. Before testing, the fiber-tab assemblies were dried in an oven at 50°C for 30 min. Tensile tests were conducted at a strain rate of 0.1 mm/min using a Universal testing machine Z10 (ZwickRoell AG, Germany) equipped with a 100 N load cell. A total of 10 specimens were tested to ensure statistical significance. The tensile strength and failure strain were recorded, and the average tensile modulus was determined from the linear region (0.2–0.3 ε_{max}) of the force-displacement curve. The crosshead displacement was used to calculate the strains, assuming a negligible contribution from machine compliance with maximum forces not exceeding 35 N. Additionally, Scanning electron microscopy (SEM) of degraded flax fibers was performed using a JSM-7500F (JEOL Ltd., Japan).

2.4 | Manufacturing of Fiber-Reinforced Polymers

A schematic illustration of the composite manufacturing process is provided in Figure 1. PMCs were fabricated using compression molding in a custom aluminum mold placed in a hydraulic hot press (Joost LAP 100, Gottfried Joos Maschinenfabrik GmbH & Co. KG, Germany). Unidirectional (UD) flax fiber mats and PA11 films, each measuring 15 cm in length and 9 cm in width, were inserted into the mold.

Prior to processing, flax mats were subjected to the temperature–time histories presented in Table 1 to achieve mass losses of 1%, 2%, 3%, 5%, and 7%, respectively, thereby specifying the state of degradation selectively. Laminates consisting of six layers of flax mats and the corresponding number of films, each with a thickness of 40 μm, were stacked to achieve a fiber weight fraction of 50 wt.-%. The approximate weight of a 6-layer laminate was determined to be 48 g based on the weight of a single fiber-mat layer (4 g) and the equivalent weight of the polymer films (4 g). A more detailed explanation of the manufacturing

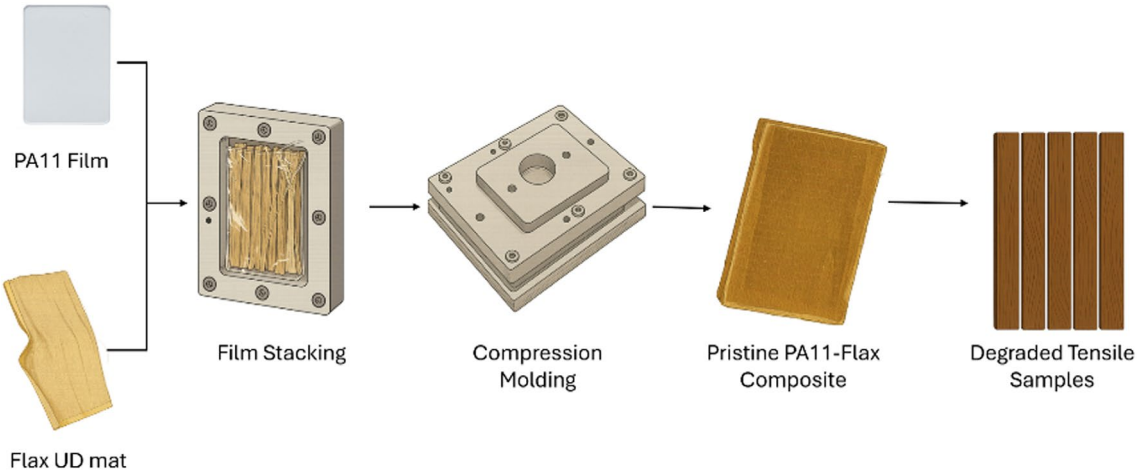

FIGURE 1 | Schematic illustration of pristine PMC manufacturing and selective degradation of the laminates.

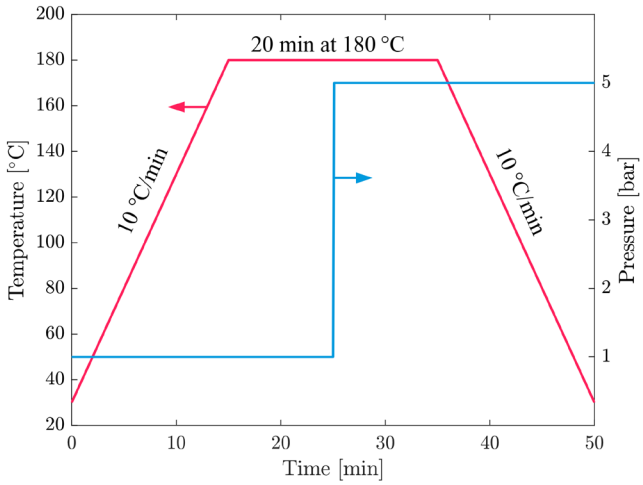

FIGURE 2 | Temperature and pressure profiles applied during laminate manufacturing.

process can be found in section 2 of the SI. The apparent fiber volume content V_f was confirmed to be 39.1 ± 2.8 vol-.% using Archimedes' principle (cf. section 3 in SI, Table S3). The total thickness of the laminate was designed to be equivalent to close to 2 mm (cf. Table S2). First, the mold was placed in a preheated hot press at 180°C for 10 min to allow for initial melting and impregnation. Subsequently, final consolidation was carried out at 180°C under a 5 bar consolidation pressure for 10 min. Cooling was performed within the hot press, maintaining the consolidation pressure throughout the cooling phase. The manufacturing cycle is shown in Figure 2. Thermocouples (Type K) were integrated in the top and mid-plane layers to record the apparent temperature profile during laminate manufacture and provide localized data for calculating degradation according to Equation (6).

2.5 | Mechanical Testing of Fiber-Reinforced Polymers

For the PMC testing, specimens measuring 120 mm in length and 15 mm in width were cut from the manufactured laminates, using Compcut ACS 600 (CompCut Advanced Composite Machining, USA) equipped with a 2 mm-wide diamond blade, and paper tabs, measuring 30 × 15 mm^2 were applied with glue to prevent slippage during testing (Figure S8). To ensure minimal fiber damage at the sides, the cutting parameters were chosen as described in section 2 of the SI. Tensile testing was performed in accordance with ASTM D3039 standard [55]. Five specimens were tested for each mass-loss percentage to achieve statistical significance. Prior to testing, all samples were dried in an oven at 80°C overnight. A crosshead gauge length of 60 mm was used to provide adequate clamping area, and an extensometer with a 30 mm gauge length was attached to the specimen surface to obtain accurate strain measurements for stiffness evaluation. Tensile tests were conducted at a strain rate of 0.1 mm/min using a Universal testing machine Z10 (ZwickRoell AG, Germany) equipped with a 20 kN load cell (Figure S9). The tensile strength and failure strain were recorded, and the average tensile modulus was determined from the linear region (0.1%–0.3%) of the force-displacement curve.

3 | Results and Discussion

3.1 | Modeling of Degradation

Figure 3a shows representative normalized mass loss and mass loss derivatives for the flax fibers and the PA11 material. Complete data are shown in Figure S10. It becomes apparent that, especially in the low-temperature regime up to 300°C, the fibers are heavily subjected to thermal degradation, while the matrix remains nearly unaffected up to temperatures of 400°C. Furthermore, prior to the central polymer degradation peak, the flax fiber exhibits initial degradation of hemicellulose and cellulose, which is already triggered at temperatures below 300°C [4] and manifests as a small peak in the normalized mass derivative located at 270°C (Figure S10b, Figure 3a). As expected, the fibers are the more temperature-sensitive constituent and require careful examination of their degradation behavior to provide appropriate temperature–time schedules for processing.

Therefore, Friedman's model-free method is applied to approximate the degradation of both the fiber and the matrix. The activation energies E_α and preexponential factor $A_\alpha f(\alpha)$ for degradation

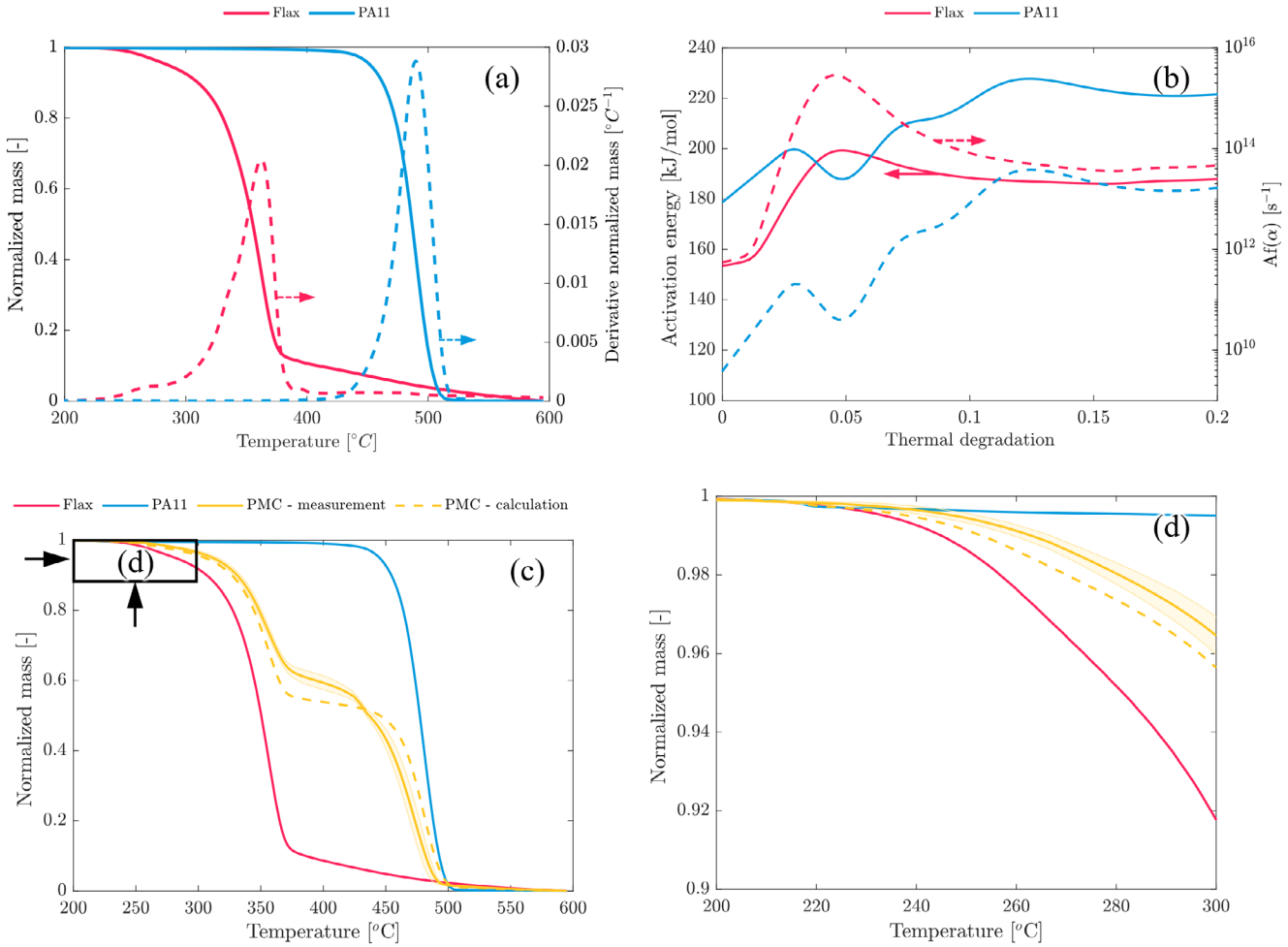

FIGURE 3 | Normalized mass and derivative normalized mass of flax fibers and PA11 at a heating rate of 15 K/min (a). Activation energy derived from isoconversional kinetics and preexponential factors for degradation states of 0 to 0.2 (b). Normalized mass for single constituents and PMC with 47.8 wt.-% (back-calculated from V_f) comparing measurement data and calculation according to the gravimetric rule of mixture (c). The region indicated in (c) is zoomed in (d).

values ranging from 0 to 0.2 are provided in (Figures 3b and S11). The activation energies of 155–200 kJ/mol and 180–230 kJ/mol for fiber and matrix materials are located in the range associated with the degradation of natural fibers [14, 25, 30] and PA11 [31] and confirm the premature degradation of the natural fibers compared with the polymeric matrix. It becomes apparent that the degradation process is subject to conversion-dependent changes and may be better approximated by apparent activation energies rather than a constant value. Average activation energies of 180 kJ mol^{-1} were reported for all degradation steps of natural fibers, suggesting that cellulose plays a significant role in Arrhenius parameters [30]. Furthermore, a comparison of experimental and model data (Figure S12) confirms good agreement for both fiber and matrix materials. Besides, the rule of mixture is applied to approximate the degradation of the composite:

$$\alpha_{FRP}(T) = W_f \alpha_f(T) + \left(1 - W_f\right)\alpha_p(T), \tag{13}$$

with α_f and α_p describing the individual gravimetric degradation of fiber and polymer material, and W_f the weight fraction of the fibers, which is calculated from V_f according to Equation S5. Figure 3c,d compare calculated data according to the gravimetric rule of mixture and measured data at a heating rate of 20 K/min. Figure S13 confirms the applicability of Equation (13), with a mean average error of < 0.5% in the temperature interval of 185°C to 343°C corresponding to 20% degradation for the mass loss and 0.015%/°C for the derivative. Interestingly, the PMC model calculation underestimates thermal degradation in the initial region (cf., Figure 3d and Figure S13). Some interactions may be beneficial and may result from the interaction of functional groups, which tend to increase temperature stability. Specific functional groups forming hydrogen bonds, dipole–dipole interactions, or even limited crosslinking with the polymer matrix might restrict chain mobility, suppress the release of low-molecular-weight volatiles, and thereby delay the onset of decomposition, resulting in an apparent increase in thermal stability. It can be concluded that considering degradation according to the rule of mixture conservatively estimates the accompanying degradation.

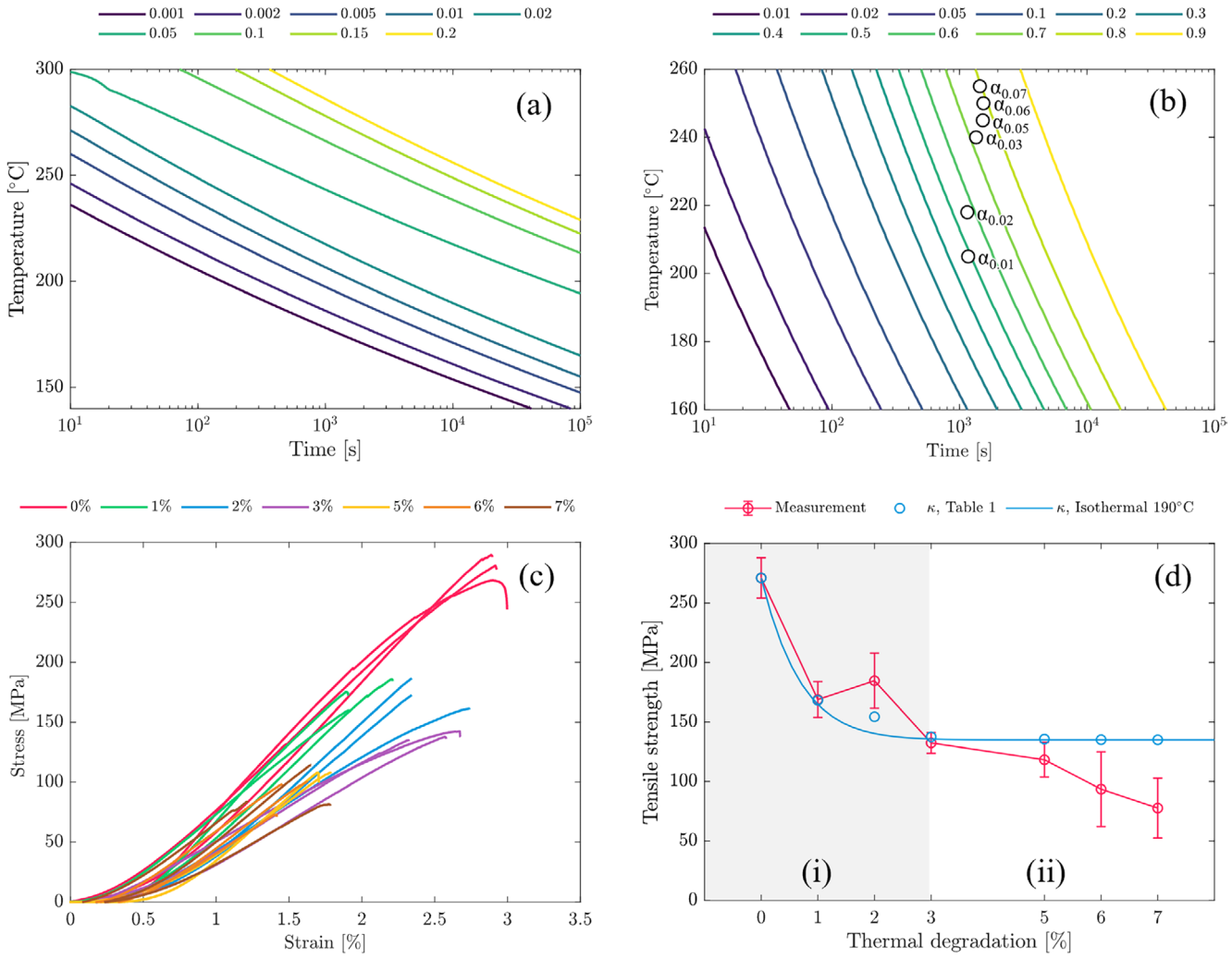

FIGURE 4 | Isoconversional lines (0.001 to 0.2) of thermal degradation α of flax fibers (a) and thermo-chemical degradation κ of flax fibers (b). Markers indicate the α values calculated from the temperature profiles provided in Table 1 (b). Stress–strain diagrams of the single fiber bundle testing (c). The number of datasets has been reduced to three for improved clarity. Measured tensile strength of flax fiber bundles at different thermal degradation states and calculated values according to the relationship from [40] (d).

Based on thermal and thermo-chemical degradation kinetics, TTT diagrams with isoconversional thermal degradation lines are derived, which enable us to read the thermal degradation that occurs when the materials are subjected to specific time–temperature profiles (Figure 4a, Figure S14). For this, Equation (6) was solved with the parameters in Figure 3b for isothermal dwellings (160°C to 260°C) up to 1E5 s, and isoconversional lines (time–temperature pairings) were interpolated. As the higher activation energies for the thermal degradation of PA11 already imply, noticeable thermal degradation of PA11 initiates at much higher temperatures (Figure S14), even above the 10% isoconversional lines of the flax fibers. Therefore, these results reaffirm that flax fibers exhibit a markedly higher temperature sensitivity, thereby constituting the principal vulnerability during processing. The TTT diagram for the thermo-chemical degradation is shown in Figure 4b and the resulting thermo-chemical degradations for the integral temperature histories provided in Table 1 are indicated. This comparison demonstrates that even small thermal degradations of 1% are accompanied by significant thermo-chemical degradation (or chain scission) of the flax fibers, making low-temperature processing rather chain-scission-dominated. In contrast, thermal degradation becomes increasingly significant at elevated temperatures. Nevertheless, within the temperature regime relevant for processing, both chain scission (i) and thermogravimetric degradation (ii) occur concurrently, rendering their individual contributions difficult to distinguish.

3.2 | Mechanical Characterization of Flax Fiber Bundles

Figure 4c,d present the mechanical testing results and evaluate the tensile strength. The derived modulus values and failure strains are provided in Figure S15. The flax fiber bundle tests confirm the continued deterioration of the mechanical properties associated with thermal degradation and chain scission. The stiffness and strength of the flax fiber bundles heavily depend on the gauge length [56], so we cannot directly apply the analytical relationship

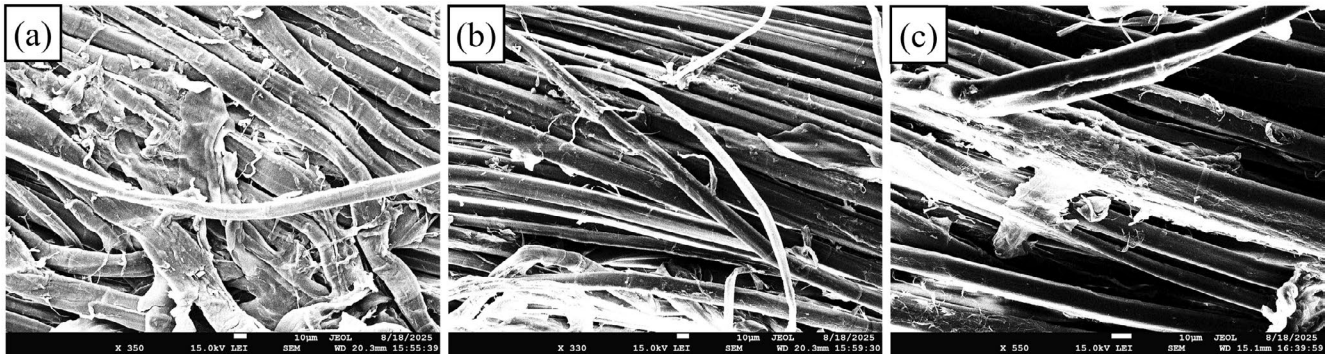

FIGURE 5 | SEM of pristine flax fibers (a) and degraded flax fibers with thermal degradation α of 2% (b) and 7% (c).

between flax fiber strength and thermo-chemical degradation as proposed in [40]. Therefore, the relationship is normalized, and the expected effect on the initial bundle strength values of 271 MPa is calculated. The thermo-chemical degradation is calculated by solving Equations (11) and (12) with the temperature profiles to achieve thermal degradations of 1%–7%, as provided in Table 1, and for isothermal continuous degradation at 190°C. Surprisingly, the measured overall deterioration of mechanical strength matches the predicted decay associated with thermo-chemical degradation ϰ up to 3% thermal degradation. A higher reduction would have been expected, given the superimposed effects of thermo-chemical and thermal material degradation. However, given the literature model for chain scission as granted, the influence of mass loss appears to be negligible up to a value of 3%, and the decay in mechanical properties can be solely explained by thermo-chemical degradation. In other words, either thermal degradation determined by gravimetry has a subordinate effect of up to 3%, which would have important implications for processing, or the literature parameters for the thermo-chemical degradation of flax fiber are not universally transferable to the underlying fiber of the present study considering batch to batch variation and degree of polymerization distribution. At higher temperatures, and upon reaching the constant limit value of the decline in mechanical properties caused by thermo-chemical material degradation, further steady thermal degradation of fiber strength occurs, characterized by weight loss exceeding 3%. Therefore, a thermal degradation of up to 3% remains within predicted range without further deteriorating the mechanical properties of flax bundles as already associated with earlier onset of chain scission (thermo-chemical degradation).

In Figure 5, elementary flax fibers can be identified in the SEM images. With increasing degradation, the fibrillar structures of the cell walls become less distinct or exhibit signs of fragmentation, resulting in a decrease in the diameter of the elementary fibers. Additionally, cortical middle lamellae, residues from the retting process, can be identified in the pristine state (Figure 5a) and become less prevalent with increasing thermo-chemical degradation. With the initial removal of waxes and leftover debris and associated irregularities at the surface of the fibers, the roughness of the fibers seems to be decreasing with increased mass loss and thermal degradation. Due to the hollow nature of the natural fibers, even though outgassing is expected, the air is removed without disruption of the surface of the fibers.

3.3 | Mechanical Properties of Flax-Reinforced PMC

During the manufacturing of flax-reinforced PMC reference laminate, temperature profiles at the part surface and in the mid-plane are recorded (Figure 6a) to calculate the resulting thermal degradation, as per Equation (13). While thermal degradation is limited to (negligible) values below 0.25%, significant chain scission of up to 40% can already be expected (cf. Figure 6b), even during the processing of the reference laminate at tool temperatures of 190°C.

Before testing, micrographs of samples from each laminate at different levels of thermal degradation were obtained to assess impregnation quality and overall condition. The optical images were captured using a VR-X-1000 confocal scanning digital microscope (Keyence Corp., Japan). Figure 7 presents representative micrographs corresponding to different thermal degradation percentages, showing a clear evolution in impregnation quality and compaction. In pristine samples, a significant number of irregular voids can be observed, which decrease progressively with increasing degradation. The presence of these voids indicates insufficient resin infiltration of the fiber network, resulting in incomplete wetting and weak interfacial bonding. At lower degradation levels, voids appear both within the fiber bundles and between individual fibers. Additionally, more gaps are observed at the interfaces between fibers, fiber bundles, and the polymer matrix, as shown in the magnified images of Figure 7. At higher percentages of thermal degradation, a gradual improvement in impregnation and compaction becomes evident. The fiber bundles appear more densely packed, with a noticeable reduction in both voids and the resin-rich regions between them. The resin appears to have effectively impregnated the fiber bundles with fewer gaps and voids present between the individual fibers. Consequently, the composite exhibits a denser, more homogeneous microstructure, indicative of improved matrix distribution and reduced interfacial defects.

Tensile testing results of the flax-reinforced PMC after selectively degrading the flax fiber are shown in (Figures 8 and S16). Only samples that failed within the gauge region, as can be seen in Figure 9a were considered for the determination of the tensile properties of the laminates. The majority of specimens exhibited failure that was dominated by fiber breakage and matrix cracking, showing cohesive failure, which can be translated into better interfacial adhesion (Figure 9a). However, some samples

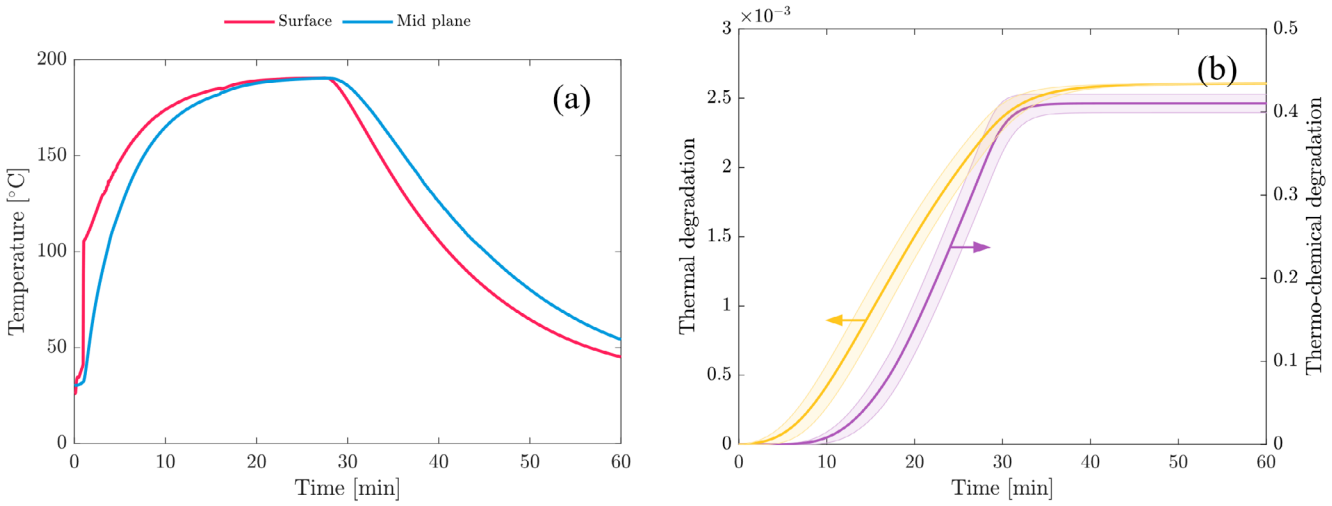

FIGURE 6 | Recorded temperature profiles during PMC manufacture (a). Average calculated thermal degradation α and thermo-chemical degradation κ according to Equations (6), (11) and (12) (b).

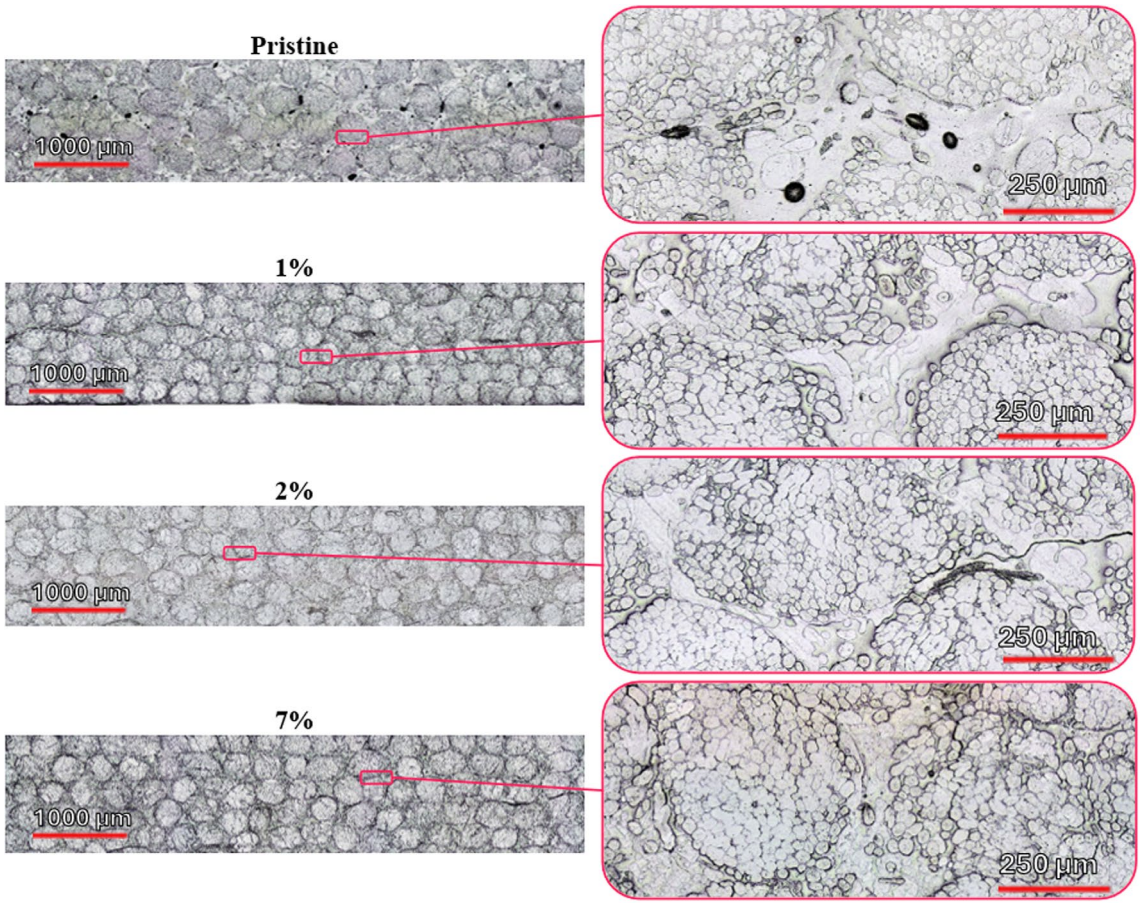

FIGURE 7 | Representative micrographs of laminates at different thermal degradation levels.

exhibit extensive fiber pull-out, interfacial debonding, and longitudinal splitting, characteristic of weaker fiber–matrix bonding and interfacial failure (Figure 9b), while others also failed at the tab location. These samples were not considered for the mechanical analysis. Similar to the neat flax fibers, the mechanical performance of the PMC decreases with increasing thermal degradation. It can be observed that the tensile properties increase slightly before showing a significant drop at a 2% degradation level. This temporary increase in fiber strength may be associated with the crosslinking of cellulose, which can be accompanied by an increase in strength. Still, an effect on the actual wetting behavior and fiber impregnation cannot be excluded. Cracking hemicellulose during selective degradation reduces the hemicellulose content and the polarity of the treated

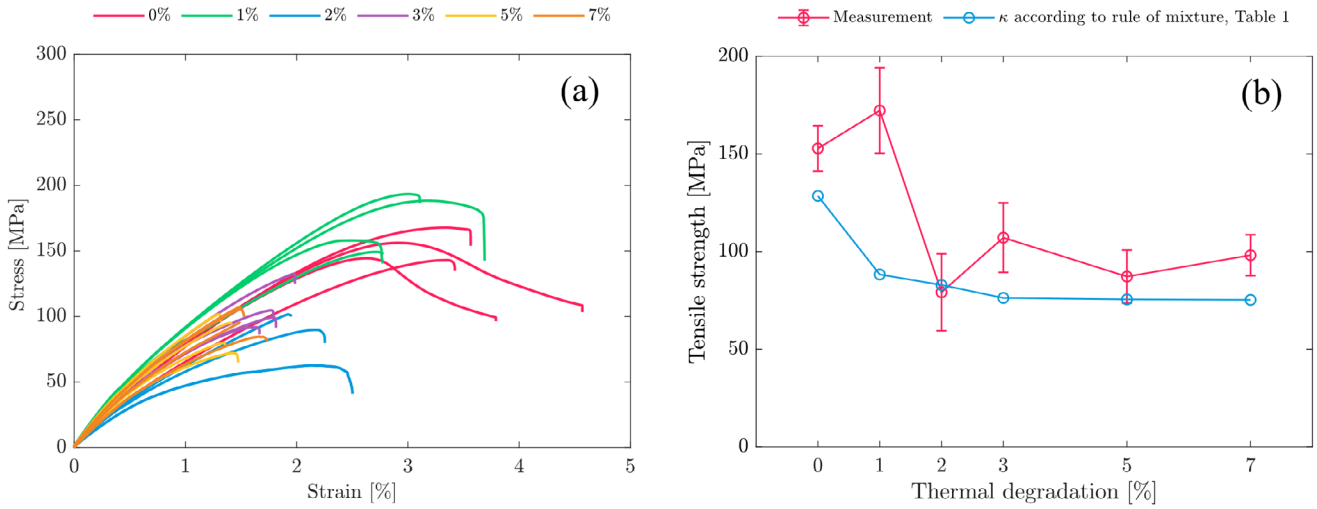

FIGURE 8 | Stress–strain diagrams of the PMC laminates tensile testing (a). Measured tensile strength of PMC laminates at different thermal degradation states a and calculated strength values according to the κ relationship from [40] and the rule of mixtures (b).

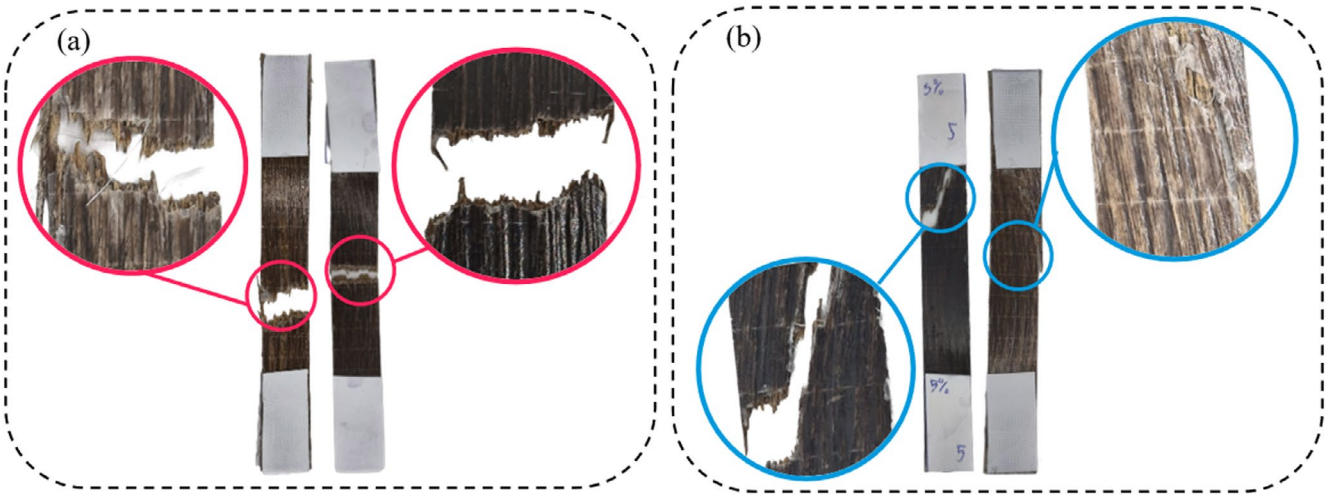

FIGURE 9 | Fracture mechanisms of representative tensile samples showing cohesive (a) and interfacial (b) fracture behavior.

flax fibers (less hydrophilic) compared with pristine fibers [57]. Therefore, degradation of the fibers up to 1% may be beneficial, as it induces better wettability and impregnation by the hydrophobic PA11 resin, resulting in improved fiber-matrix adhesion and higher strength values. Besides that, the fiber surface becomes smoother as thermal degradation initiates (Figure 5c), which diminishes wetting by decreasing the total available surface area and reducing the interaction with the liquid.

By applying the volumetric rule of mixture (cf. Equation (13)) with an average fiber volume content of 39.1 vol.-% and a tensile strength of 32 MPa [58] of the PA11 material, the composite tensile strength is calculated according to the relationship from [40], demonstrating a reasonable agreement with the measurement data (Figure 8b).

Still, the Flax PMCs exhibit lower strength compared with expected literature values. Owing to the low processing temperatures, any influence of matrix degradation and apparent scission can be neglected. The effect of gauge length may explain this underestimation, as strength tends to decrease with increasing gauge length [56]. While initial bundle strength values of 271 MPa were measured at an 80 mm gauge length, the PMCs were tested at a 30 mm gauge length. Only specimens with failure within the gauge length were considered valid. The pristine strength values are located in the range of literature values [59] for unidirectional flax with PA11 matrix, considering the lower fiber volume contents in the present study. One exception is the counterintuitive increase in strength at 1% thermal degradation, which is not covered in the correlation from [40] and may be associated with the proposed effect of improved fiber-matrix adhesion, facilitating the impregnation process. Besides tensile strength, elongation at break decreases steadily, while stiffness remains relatively unaffected (Figure S16).

Compiling the results of mechanical testing into the previously introduced TTS diagram enables us to identify distinct processing regimes (i)–(iii) for the manufacturing of flax fiber PMCs. Region (i) in Figure 10 indicates the secure processing

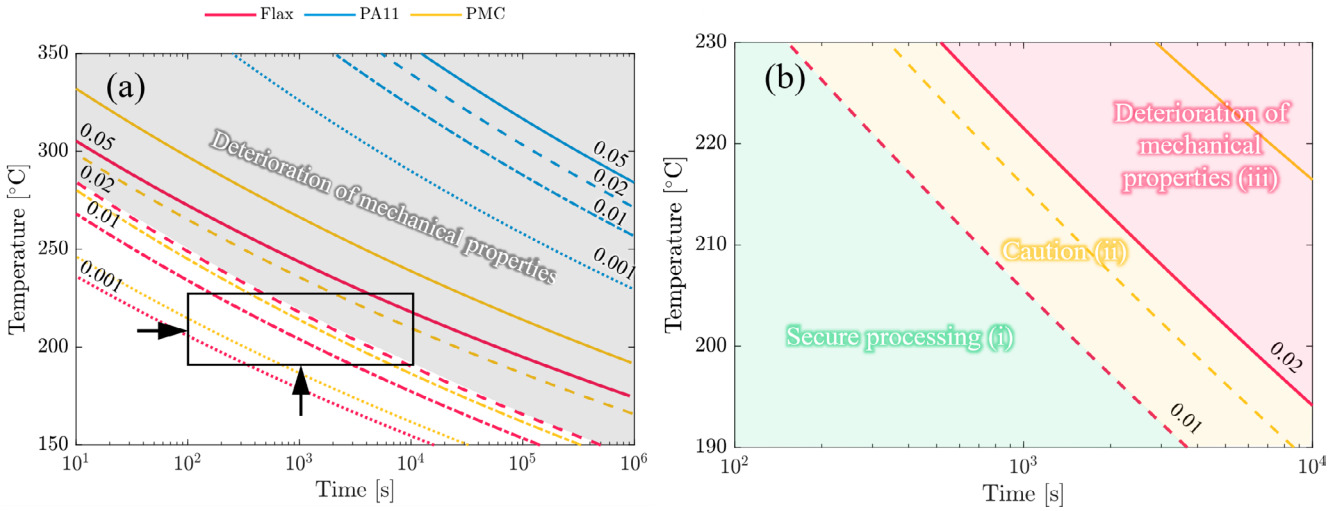

FIGURE 10 | Combined isoconversional degradation lines of flax fibers, PA11, and PMC (a) and zoom in on distinct processing regions without significant deterioration of mechanical properties (b).

window, which can be accompanied by improved fiber impregnation, yielding better adhesion and PMC tensile strength. Even though significant thermo-chemical degradation can already be expected (Figure 4b) in this range, the impact on mechanical property breakdown remains limited, as it's partly compensated by better fiber impregnation. Beyond selecting the nominal processing temperature, maintaining precise temperature control is crucial, as deviations of 10°C or more may already drive the system from the safe into the more critical processing regime (cf. Figure S17). Region (ii) warrants a cautious approach, as it may be accompanied by a detrimental reduction in mechanical properties, depending on whether the individual degradation of the fiber bundles or thermogravimetric degradation of the PMC according to the rule of mixture represents the data basis for setting the isoconversional lines.

In region (iii), the PMC undergoes significant thermal and thermo-chemical degradation, resulting in a detrimental reduction in mechanical performance, which is to be categorically avoided in the processing of PMCs.

4 | Conclusion

In this paper, we link the thermal and thermo-chemical degradation of flax fiber bundles and flax fiber–reinforced bio-PMC during thermal processing with their mechanical properties. Thermo-chemical degradation by chain scission initiates well before thermogravimetric degradation, and weight reductions of 1% already cause a significant degradation in the mechanical performance of the reinforcing flax fibers, thus highlighting the necessity of precise temperature control. In PMC, a slight degradation may be desirable, as a 15% increase in tensile strength is reported at 1% thermal degradation, which may be due to improved fiber-matrix adhesion caused by enhanced wetting behavior.

A Framework for deriving processing maps for thermoplastic PMC based on PA11 and flax fibers is introduced, comprising thermal degradation kinetic modeling and determination of the resulting mechanical properties of the flax fibers and manufactured composites. By linking thermal degradation to deterioration in mechanical properties, a threshold can be identified beyond which the degradation becomes detrimental to mechanical performance, thereby constraining the allowable processing window. The parameterized kinetic model enables flexible mapping of various arbitrary temperature cycles while ensuring that the degradation threshold is not exceeded. The derived framework thereby facilitates transferability to diverse processing conditions and heat-treatment protocols. It may be applied to varying fiber and matrix systems, thereby providing an expanded basis for systematic investigations into bio-based PMC and fibers for advanced composite applications. However, these processing conditions must be carefully balanced against the resin's flow behavior (for good fiber impregnation) and potential delays arising from heat equilibration processes such as heat-up, thereby constituting a coupled multi-physics problem. Further work may focus on more thoroughly characterizing the 0%–2% thermal degradation region to identify the beneficial effects of processing. Additionally, no chain-scission model for PA11 is currently available, which could make a vital contribution to a more comprehensive understanding of thermal degradation in the production of bio PMC.

Author Contributions

Dimitrios Apostolidis: investigation, methodology, visualization, writing – original draft. **Prajwal Jayaraman:** investigation, writing – review and editing. **Clemens A. Dransfeld:** conceptualization, funding acquisition, writing – review and editing. **Baris Kumru:** funding acquisition, writing – review and editing. **Niklas Lorenz:** conceptualization, methodology, data curation, investigation, writing – review and editing, writing – original draft, visualization.

Acknowledgments

This project is made possible partly by a contribution from the National Growth Fund program NXTGEN HIGHTECH 01 (NGFNH2201) and from Luchtvaart en Transitie (LiT). The authors acknowledge continuous support from the ASM department and technical staff.

Funding

This work was supported by Luchtvaart en Transitie (LiT). National Growth Fund program NXTGEN HIGHTECH 01 (NGFNH2201).

Conflicts of Interest

The authors declare no conflicts of interest.

Data Availability Statement

The data that support the findings of this study are available from the corresponding author upon reasonable request.

References

1. M. Winnacker and B. Rieger, "Biobased Polyamides: Recent Advances in Basic and Applied Research," *Macromolecular Rapid Communications* 37, no. 17 (2016): 1391–1413, https://doi.org/10.1002/marc.201600181.

2. H. L. Ornaghi, M. Poletto, A. J. Zattera, and S. C. Amico, "Correlation of the Thermal Stability and the Decomposition Kinetics of Six Different Vegetal Fibers," *Cellulose* 21, no. 1 (2014): 177–188, https://doi.org/10.1007/s10570-013-0094-1.

3. L. Yan, N. Chouw, and K. Jayaraman, "Flax Fibre and Its Composites – A Review," *Composites Part B: Engineering* 56 (2014): 296–317, https://doi.org/10.1016/j.compositesb.2013.08.014.

4. S. Kumar, L. Prasad, P. P. Bijlwan, and A. Yadav, "Thermogravimetric Analysis of Lignocellulosic Leaf-Based Fiber-Reinforced Thermosets Polymer Composites: An Overview," *Biomass Conversion and Biorefinery* 14, no. 12 (2024): 12673–12698, https://doi.org/10.1007/s13399-022-03332-0.

5. S. Islam, M. B. Hasan, F. E. Karim, et al., "Thermoset and Thermoplastic Polymer Composites Reinforced With Flax Fiber: Properties and Application—A Review," *SPE Polymers* 6, no. 1 (2025): e10172, https://doi.org/10.1002/pls2.10172.

6. H. M. Khanlou, P. Woodfield, J. Summerscales, and W. Hall, "Consolidation Process Boundaries of the Degradation of Mechanical Properties in Compression Moulding of Natural-Fibre Bio-Polymer Composites," *Polymer Degradation and Stability* 138 (2017): 115–125, https://doi.org/10.1016/j.polymdegradstab.2017.03.004.

7. J. L. Thomason and J. L. Rudeiros-Fernández, "Thermal Degradation Behaviour of Natural Fibres at Thermoplastic Composite Processing Temperatures," *Polymer Degradation and Stability* 188 (2021): 109594, https://doi.org/10.1016/j.polymdegradstab.2021.109594.

8. G. Parodo, L. Sorrentino, S. Turchetta, and G. Moffa, "Manufacturing of Sustainable Composite Materials: The Challenge of Flax Fiber and Polypropylene," *Materials (Basel)* 17, no. 19 (2024): 4768, https://doi.org/10.3390/ma17194768.

9. J. George, E. T. J. Klompen, and T. Peijs, "Thermal Degradation of Green and Upgraded Flax Fibres," *Advanced Composites Letters* 10, no. 2 (2001): 096369350101000205, https://doi.org/10.1177/096369350101000205.

10. J. Gassan and A. K. Bledzki, "Thermal Degradation of Flax and Jute Fibers," *Journal of Applied Polymer Science* 82, no. 6 (2001): 1417–1422, https://doi.org/10.1002/app.1979.

11. A. V. Rajulu, R. R. Devi, and L. G. Devi, "Thermal Degradation Parameters of Bamboo Fiber Reinforcement," *Journal of Reinforced Plastics and Composites* 24, no. 13 (2005): 1407–1411, https://doi.org/10.1177/0731684405049883.

12. R. Herrera, X. Erdocia, R. Llano-Ponte, and J. Labidi, "Characterization of Hydrothermally Treated Wood in Relation to Changes on Its Chemical Composition and Physical Properties," *Journal of Analytical and Applied Pyrolysis* 107 (2014): 256–266, https://doi.org/10.1016/j.jaap.2014.03.010.

13. F. Guo, X. Zhang, R. Yang, L. Salmén, and Y. Yu, "Hygroscopicity, Degradation and Thermal Stability of Isolated Bamboo Fibers and Parenchyma Cells Upon Moderate Heat Treatment," *Cellulose* 28, no. 13 (2021): 8867–8876, https://doi.org/10.1007/s10570-021-04050-y.

14. K. Van De Velde and P. Kiekens, "Thermal Degradation of Flax: The Determination of Kinetic Parameters With Thermogravimetric Analysis," *Journal of Applied Polymer Science* 83, no. 12 (2002): 2634–2643, https://doi.org/10.1002/app.10229.

15. M. C. Popescu, C. M. Popescu, G. Lisa, and Y. Sakata, "Evaluation of Morphological and Chemical Aspects of Different Wood Species by Spectroscopy and Thermal Methods," *Journal of Molecular Structure* 988, no. 1 (2011): 65–72, https://doi.org/10.1016/j.molstruc.2010.12.004.

16. J. J. M. Orfão, F. J. A. Antunes, and J. L. Figueiredo, "Pyrolysis Kinetics of Lignocellulosic Materials—Three Independent Reactions Model," *Fuel* 78, no. 3 (1999): 349–358, https://doi.org/10.1016/S0016-2361(98)00156-2.

17. C. Di Blasi, "Modeling Chemical and Physical Processes of Wood and Biomass Pyrolysis," *Progress in Energy and Combustion Science* 34, no. 1 (2008): 47–90, https://doi.org/10.1016/j.pecs.2006.12.001.

18. C. H. Yeh and T. C. Yang, "Utilization of Waste Bamboo Fibers in Thermoplastic Composites: Influence of the Chemical Composition and Thermal Decomposition Behavior," *Polymers* 12, no. 3 (2020): 636, https://doi.org/10.3390/polym12030636.

19. M. Protim Mudoi and S. Sinha, "Thermal Degradation Study of Natural Fibre Through Thermogravimetric Analysis," *Materials Today: Proceedings* 99 (2024): 92–97, https://doi.org/10.1016/j.matpr.2023.05.362.

20. S. Vigneshwaran, R. Sundarakannan, K. M. John, et al., "Recent Advancement in the Natural Fiber Polymer Composites: A Comprehensive Review," *Journal of Cleaner Production* 277 (2020): 124109, https://doi.org/10.1016/j.jclepro.2020.124109.

21. S. Liang, H. Nouri, and E. Lafranche, "Thermo-Compression Forming of Flax Fibre-Reinforced Polyamide 6 Composites: Influence of the Fibre Thermal Degradation on Mechanical Properties," *Journal of Materials Science* 50, no. 23 (2015): 7660–7672, https://doi.org/10.1007/s10853-015-9330-4.

22. K. Van de Velde and E. Baetens, "Thermal and Mechanical Properties of Flax Fibres as Potential Composite Reinforcement," *Macromolecular Materials and Engineering* 286, no. 6 (2001): 342–349, https://doi.org/10.1002/1439-2054(20010601)286:6<342::AID-MAME342>3.0.CO;2-P.

23. J. Chaishome, K. A. Brown, R. Brooks, and M. J. Clifford, "Thermal Degradation of Flax Fibres as Potential Reinforcement in Thermoplastic Composites," *Advanced Materials Research* 894 (2014): 32–36, https://doi.org/10.4028/www.scientific.net/AMR.894.32.

24. A. Bourmaud, A. Le Duigou, C. Gourier, and C. Baley, "Influence of Processing Temperature on Mechanical Performance of Unidirectional Polyamide 11–Flax Fibre Composites," *Industrial Crops and Products* 84 (2016): 151–165, https://doi.org/10.1016/j.indcrop.2016.02.007.

25. B. Wielage, T. Lampke, G. Marx, K. Nestler, and D. Starke, "Thermogravimetric and Differential Scanning Calorimetric Analysis of Natural Fibres and Polypropylene," *Thermochimica Acta* 337, no. 1 (1999): 169–177, https://doi.org/10.1016/S0040-6031(99)00161-6.

26. G. Testa, A. Sardella, E. Rossi, C. Bozzi, and A. Seves, "The Kinetics of Cellulose Fiber Degradation and Correlation With Some Tensile Properties," *Acta Polymerica* 45, no. 1 (1994): 47–49, https://doi.org/10.1002/actp.1994.010450109.

27. P. Das and P. Tiwari, "Thermal Degradation Kinetics of Plastics and Model Selection," *Thermochimica Acta* 654 (2017): 191–202, https://doi.org/10.1016/j.tca.2017.06.001.

28. S. Vyazovkin, *Isoconversional Kinetics of Thermally Stimulated Processes* (Springer International Publishing, 2015).

29. N. Lorenz, W. E. Dyer, and B. Kumru, "Thermo-Rheological and Kinetic Characterization and Modeling of an Epoxy Vitrimer Based on Polyimine Exchange," *Soft Matter* 20 (2024): 10.1039.D4SM00724G, https://doi.org/10.1039/D4SM00724G.

30. H. L. Ornaghi, F. G. Ornaghi, K. C. C. de Carvalho Benini, and O. Bianchi, "A Comprehensive Kinetic Simulation of Different Types of Plant Fibers: Autocatalytic Degradation Mechanism," *Cellulose* 26, no. 12 (2019): 7145–7157, https://doi.org/10.1007/s10570-019-02610-x.

31. L. Ferry, R. Sonnier, J. M. Lopez-Cuesta, S. Petigny, and C. Bert, "Thermal Degradation and Flammability of Polyamide 11 Filled With Nanoboehmite," *Journal of Thermal Analysis and Calorimetry* 129, no. 2 (2017): 1029–1037, https://doi.org/10.1007/s10973-017-6244-1.

32. H. L. Friedman, "Kinetics of Thermal Degradation of Char-Forming Plastics From Thermogravimetry. Application to a Phenolic Plastic," *Journal of Polymer Science Part C: Polymer Symposia* 6, no. 1 (1964): 183–195, https://doi.org/10.1002/polc.5070060121.

33. P. Rajeshwari and T. K. Dey, "Advanced Isoconversional and Master Plot Analyses on Non-Isothermal Degradation Kinetics of AlN (Nano)-Reinforced HDPE Composites," *Journal of Thermal Analysis and Calorimetry* 125, no. 1 (2016): 369–386, https://doi.org/10.1007/s10973-016-5406-x.

34. S. Vyazovkin and C. A. Wight, "Isothermal and Non-Isothermal Kinetics of Thermally Stimulated Reactions of Solids," *International Reviews in Physical Chemistry* 17, no. 3 (1998): 407–433, https://doi.org/10.1080/014423598230108.

35. Y. Dobah, I. Zampetakis, C. Ward, and F. Scarpa, "Thermoformability Characterisation of Flax Reinforced Polypropylene Composite Materials," *Composites Part B: Engineering* 184 (2020): 107727, https://doi.org/10.1016/j.compositesb.2019.107727.

36. K. de Van Vel and P. Kiekens, "Effect of Material and Process Parameters on the Mechanical Properties of Unidirectional and Multidirectional Flax/Polypropylene Composites," *Composite Structures* 62, no. 3 (2003): 443–448, https://doi.org/10.1016/j.compstruct.2003.09.018.

37. S. Alimuzzaman, R. H. Gong, and M. Akonda, "Nonwoven Polylactic Acid and Flax Biocomposites," *Polymer Composites* 34, no. 10 (2013): 1611–1619, https://doi.org/10.1002/pc.22561.

38. N. Lorenz, K. Fischer, and C. Hopmann, "Surface Waviness of Continuous Fiber-Reinforced Polymer Composites – a Review on Their Formation, Characterization and Modeling," *Composites Part A: Applied Science and Manufacturing* 198 (2025): 109067, https://doi.org/10.1016/j.compositesa.2025.109067.

39. I. M. De Rosa, J. M. Kenny, D. Puglia, C. Santulli, and F. Sarasini, "Morphological, Thermal and Mechanical Characterization of Okra (*Abelmoschus esculentus*) Fibres as Potential Reinforcement in Polymer Composites," *Composites Science and Technology* 70, no. 1 (2010): 116–122, https://doi.org/10.1016/j.compscitech.2009.09.013.

40. H. M. Khanlou, P. Woodfield, J. Summerscales, et al., "Estimation of Mechanical Property Degradation of Poly(Lactic Acid) and Flax Fibre Reinforced Poly(Lactic Acid) Bio-Composites During Thermal Processing," *Measurement* 116 (2018): 367–372, https://doi.org/10.1016/j.measurement.2017.11.031.

41. A. Arbelaiz, B. Fernández, J. A. Ramos, and I. Mondragon, "Thermal and Crystallization Studies of Short Flax Fibre Reinforced Polypropylene Matrix Composites: Effect of Treatments," *Thermochimica Acta* 440, no. 2 (2006): 111–121, https://doi.org/10.1016/j.tca.2005.10.016.

42. M. Poletto, H. L. O. Júnior, and A. J. Zattera, "Thermal Decomposition of Natural Fibers: Kinetics and Degradation Mechanisms," in *Reactions and Mechanisms in Thermal Analysis of Advanced Materials*, 1st ed., ed. A. Tiwari and B. Raj (Wiley, 2015), 515–545, https://doi.org/10.1002/9781119117711.ch21.

43. P. Tranchard, S. Duquesne, F. Samyn, B. Estèbe, and S. Bourbigot, "Kinetic Analysis of the Thermal Decomposition of a Carbon Fibre-Reinforced Epoxy Resin Laminate," *Journal of Analytical and Applied Pyrolysis* 126 (2017): 14–21, https://doi.org/10.1016/j.jaap.2017.07.002.

44. N. Sbirrazzuoli, "Determination of Pre-Exponential Factors and of the Mathematical Functions f(α) or G(α) That Describe the Reaction Mechanism in a Model-Free Way," *Thermochimica Acta* 564 (2013): 59–69, https://doi.org/10.1016/j.tca.2013.04.015.

45. C. K. Tziamtzi and K. Chrissafis, "Optimization of a Commercial Epoxy Curing Cycle via DSC Data Kinetics Modelling and TTT Plot Construction," *Polymer* 230 (2021): 124091, https://doi.org/10.1016/j.polymer.2021.124091.

46. S. Vyazovkin, A. K. Burnham, J. M. Criado, L. A. Pérez-Maqueda, C. Popescu, and N. Sbirrazzuoli, "ICTAC Kinetics Committee Recommendations for Performing Kinetic Computations on Thermal Analysis Data," *Thermochimica Acta* 520, no. 1–2 (2011): 1–19, https://doi.org/10.1016/j.tca.2011.03.034.

47. H. E. Kissinger, "Reaction Kinetics in Differential Thermal Analysis," *Analytical Chemistry* 29, no. 11 (1957): 1702–1706, https://doi.org/10.1021/ac60131a045.

48. T. Ozawa, "A New Method of Analyzing Thermogravimetric Data," *Bulletin of the Chemical Society of Japan* 38, no. 11 (1965): 1881–1886, https://doi.org/10.1246/bcsj.38.1881.

49. J. H. Flynn and L. A. Wall, "A Quick, Direct Method for the Determination of Activation Energy From Thermogravimetric Data," *Journal of Polymer Science Part B: Polymer Letters* 4, no. 5 (1966): 323–328, https://doi.org/10.1002/pol.1966.110040504.

50. S. Vyazovkin, "Advanced Isoconversional Method," *Journal of Thermal Analysis* 49, no. 3 (1997): 1493–1499, https://doi.org/10.1007/bf01983708.

51. J. Farjas and P. Roura, "Isoconversional Analysis of Solid-State Transformations: A Critical Review. Part III. Isothermal and Non Isothermal Predictions," *Journal of Thermal Analysis and Calorimetry* 109, no. 1 (2012): 183–191, https://doi.org/10.1007/s10973-011-1642-2.

52. D. Sanchez-Rodriguez, S. Zaidi, Y. Jahani, et al., "Processability and Reprocessability Maps for Vitrimers Considering Thermal Degradation and Thermal Gradients," *Polymer Degradation and Stability* 217 (2023): 110543, https://doi.org/10.1016/j.polymdegradstab.2023.110543.

53. J. Morales, R. M. Michell, and D. Rodrigue, "Impact of Mechanical Reprocessing on Degradation and Performance of PA 11 and PA 11–LDPE Blends," *Polymer Degradation and Stability* 241 (2025): 111541, https://doi.org/10.1016/j.polymdegradstab.2025.111541.

54. ASTM International, "ASTM C1557–20, Standard Test Method for Tensile Strength and Young's Modulus of Fibers," 2020, https://compass.astm.org/content-access?contentCode=ASTM%7CC1557-20%7Cen-US.

55. ASTM International, "ASTM D3039/D3039M-08, Standard Test Method for Tensile Properties of Polymer Matrix Composite Materials," 2014, https://compass.astm.org/content-access?contentCode=ASTM%7CD3039_D3039M-08%7Cen-US.

56. M. Chalard, F. Bedel, C. Buffet, et al., "Analysis of the Tensile Behaviour of Flax Fibre Bundles as a Function of the Loaded Volume," *Composites Part A: Applied Science and Manufacturing* 190 (2025): 108704, https://doi.org/10.1016/j.compositesa.2024.108704.

57. M. F. Pucci, P. J. Liotier, D. Seveno, C. Fuentes, A. Van Vuure, and S. Drapier, "Wetting and Swelling Property Modifications of Elementary Flax Fibres and Their Effects on the Liquid Composite Molding Process," *Composites Part A: Applied Science and Manufacturing* 97 (2017): 31–40, https://doi.org/10.1016/j.compositesa.2017.02.028.

58. Arkema S.A, "Technical Data Sheet, Rilsan PA11, Arkema," Technical Data Sheet, Rilsan PA11.

59. C. Gourier, A. Bourmaud, A. Le Duigou, and C. Baley, "Influence of PA11 and PP Thermoplastic Polymers on Recycling Stability of Unidirectional Flax Fibre Reinforced Biocomposites," *Polymer Degradation and Stability* 136 (2017): 1–9, https://doi.org/10.1016/j.polymdegradstab.2016.12.003.

Supporting Information

Additional supporting information can be found online in the Supporting Information section. **Data S1:** Supporting Information.